The Plant Cell, Vol. 24: 4149–4162, October 2012, www.plantcell.org

The Spectrum and Frequency of Self-Inflicted and Host Gene Mutations Produced by the Transposon *Ac* in Maize[C][W]

Jun T. Huang[a,b] and Hugo K. Dooner[a,b,1]

[a] Waksman Institute, Rutgers University, Piscataway, New Jersey 08854
[b] Department of Plant Biology, Rutgers University, New Brunswick, New Jersey 08901

The autonomous transposon *Activator* (*Ac*) is a powerful mutagen. *Ac*-induced mutations range from small footprints of host sequences to large rearrangements of transposon or host sequences. These mutations arise by different repair mechanisms of the double-strand break produced by *Ac* excision: footprints by nonhomologous end joining and rearrangements by various mechanisms, including DNA replication repair. Footprints greatly outnumber other mutations, masking them because they usually share a nonfunctional phenotype. To determine the spectrum and frequencies of host and self-mutations generated by *Ac*, we used an allele harboring *Ac* in the 5′ untranslated region *bronze* (*bz*). In this system, simple excisions produce purple revertants, whereas deletions of host or transposon sequences produce stable bronze (bz-s) mutants. Internal and terminal deletions of *Ac* predominated among the 72 bz-s derivatives. Most internal deletions (52 of 54) behaved as nonautonomous *Dissociation* (*Ds*) elements. All nine terminal deletions or *fractured Ac* (*fAc*) elements had rearrangements of adjacent host sequences. Most *Ds* and *fAc* deletion junctions displayed microhomologies and contained filler DNA from nearby sequences, suggesting an origin by DNA repair synthesis followed by microhomology-mediated end joining. All mutations occurred more frequently in pollen, where one in 200 grains carried new *Ds* or *fAc* elements.

INTRODUCTION

Activator (*Ac*) was the first autonomous or self-mobile transposable element (TE) described by McClintock (1949). In addition to itself, *Ac* can mobilize its nonautonomous *Dissociation* (*Ds*) counterparts, which share common ends with it but do not encode a transposase. *Ac* and *Ds* belong to the *hAT* superfamily of DNA TEs (Kunze and Weil, 2002). *Ac* is 4565 bp long and has 11-bp imperfect terminal inverted repeats (TIRs) and ~240-bp subterminal regions at both ends, which are essential for transposition (Coupland et al., 1989). The central region of *Ac* encodes a transposase that is both necessary and sufficient to mobilize *Ac* and *Ds* elements in various transgenic organisms that lack *Ac*-homologous sequences (Coupland et al., 1988).

Ac and *Ds* are the best-studied plant *hAT* transposons, and their detailed analysis has allowed a glimpse of some of the genetic interactions that are possible between transposons of that superfamily and their hosts (Dooner and Weil, 2012). *Ac* is a potent, versatile, and indiscriminate mutagen that has coevolved with its maize (*Zea mays*) host. It is potent because it causes mutations in a high percentage of gametes, versatile because it can induce various kinds of mutations, and indiscriminate because it does not differentiate between its own DNA and that of the host. Like most other DNA transposons, *Ac* transposes by a cut-and-paste mechanism. It is the ability to frequently cut itself from the linear continuity of the chromosome by introducing double-strand breaks (DSBs) that makes *Ac* a powerful mutagen. The subsequent repair of these DSBs by the host's enzymatic machinery rarely leaves the DNA in its pristine condition, but leads instead to a variety of changes, from the addition or deletion of a few bp to large-scale chromosomal rearrangements, all of which have the potential to generate diversity.

Insertion of *Ac* causes the duplication of 8 bp of host sequence on either side of *Ac* (target site duplication [TSD]). Excision of *Ac* generates a DSB that is repaired predominantly by the nonhomologous end joining (NHEJ) pathway, which leaves behind excision footprints of variable size and composition (Scott et al., 1996; Rubin and Levy, 1997; Huefner et al., 2011). *Ac* tends to insert in coding regions (Cowperthwaite et al., 2002); therefore, these excision footprints often disrupt the normal reading frame of the gene and lead to nonfunctional alleles.

Other types of mutations can be produced by repair of the DSBs caused by *Ac* excision, but at much lower frequencies. The most common of these is mutation to *Ds*. Unlike the highly conserved *Ac*, *Ds* elements are structurally diverse, but many are simple internal deletion derivatives of various sizes. McClintock (1956, 1962, 1963) reported several cases at the *wx* and *bz* loci in which *Ac* appeared to have mutated to *Ds*, and later molecular analysis proved them to be internal deletions of *Ac* (Pohlman et al., 1984; Dooner et al., 1986; Yan et al., 1999). Similar mutations of *Ac* to *Ds* were subsequently described at *bz*, *ps1*, and other loci (Yan et al., 1999; Conrad et al., 2007). Less frequently, *Ac* can cause a large deletion of adjacent host sequences. Derivative *bz-s*:*2114*(*Ac*) from the maize mutable allele *bz-m2*(*Ac*) lost 789 bp of *bz* sequence adjacent to the 5′ end of *Ac*; however, the transposition frequency of *Ac2114*,

[1] Address correspondence to dooner@waksman.rutgers.edu.
The author responsible for distribution of materials integral to the findings presented in this article in accordance with the policy described in the Instructions for Authors (www.plantcell.org) is: Hugo K. Dooner (dooner@waksman.rutgers.edu).
[C] Some figures in this article are displayed in color online but in black and white in the print edition.
[W] Online version contains Web-only data.
www.plantcell.org/cgi/doi/10.1105/tpc.112.104265

which is not flanked by a TSD, was not affected (Dooner et al., 1988). A second rare *Ac* rearrangement was reported by Ralston et al. (1989) in the *bz-s2094* derivative from *bz-m2*(*Ac*), which displayed a remarkable propensity to break chromosomes. The 3′ end of *Ac* and the adjacent *bz* sequence in this allele are identical to the parental line, but various rearrangements occurred at the 5′ end. *bz-s2094* carries a *fractured Ac* (*fAc*), which lost 2 kb from its 5′ end, adjacent to a 37-bp duplication of host sequence and a typical *Ac* excision footprint. Similar *fAc* elements retaining only the 3′ end have also been described at *P1* by Zhang and Peterson (2004) and at *ps1* by Conrad et al. (2007). The spectrum and frequencies of the more rare null mutations are difficult to ascertain because of the overwhelming number of simple excision products that have the same null mutant phenotype. Conrad et al. (2007) analyzed 753 kernels with a mutant phenotype from several *Ac* donor lines and found only 24 such *Ac* inactivation events. The system that we report on here is highly efficient for isolating these more rare events, which most likely arise from DSB repair by an error-prone DNA synthesis pathway and from aberrant transpositions.

bz-m39(*Ac*) is a mutable allele harboring an *Ac* element in the 5′ untranslated region (UTR) of the *bz* gene, 32 to 39 bp upstream of the start codon. The transposon footprints generated by *Ac39* excision in the *bz* 5′ UTR do not interfere with gene function; therefore, all simple excisions produce purple (Bz') revertants, rather than stable bronze (bz-s) derivatives. We took advantage of this property to set up an efficient screen for the rare *Ac* deletion mutations. We isolated 72 exceptional bz-s derivatives and found various types of transposon and host gene mutations. Internal deletions of *Ac* constituted the majority class. Most of the 54 deletions behaved as new *Ds* elements, because they could be mobilized by *Ac* in trans. Surprisingly, given just three sporadic instances in the literature, nine *fAc*s were found in this study, making them the second most abundant class of bz-s derivatives. The *fAc* elements, which can retain either the 5′ or 3′ end, were always accompanied by either duplications or deletions of adjacent host sequences. The remaining nine bz-s mutants fell into various classes: seven adjacent deletions with or without *Ac*, one hypermethylated cycling *Ac*, and one coincidental *Magellan* long terminal repeat (LTR) retrotransposon insertion. This study provides a comprehensive view of the types and frequencies of mutations, other than simple excision footprints, that can be produced at a locus by different repair of *Ac*-induced DSBs.

RESULTS

Simple Excisions versus Complex Mutations of *Ac*

Complex mutations of *Ac*-mutable alleles are difficult to identify phenotypically, because they are greatly outnumbered by the *Ac* simple excision footprints with which they usually share the same loss-of-instability diagnostic phenotype. The *bz-m39*(*Ac*) system allows us to efficiently select for such mutations. The *Ac* element in the *bz-m39*(*Ac*) allele excises frequently in somatic tissues, producing heavily variegated kernel and plant phenotypes (Figure 1). The *Ac39* excision footprints in the *bz* 5′ UTR should not interfere with gene function, so all simple germinal excisions should produce purple kernel (Bz′) revertants. By contrast, bz-s mutations should be derived from more complex mutations that disrupt expression of the *bz* gene.

To select both Bz′ and bz-s mutations, *bz-m39*(*Ac*) hemizygotes were backcrossed as either male or female parents to *sh-bz-X2*, a line carrying a large x-ray–induced deletion of the 2-centimorgan*sh-bz* interval on *9S* (Table 1). A total of 72 bz-s mutants were recovered: 11 from 5690 female gametes, and 61 from 11,870 male gametes. By comparison, a similar number of *Ac39* simple excision derivatives could be obtained from a much smaller population. A total of 78 Bz′ (purple) revertants with typical transposon footprints were recovered from just more than 1000 *bz-m39*(*Ac*) gametes: 25 from 466 female gametes, and 53 from 550 male gametes. Twelve classes of transposon footprints were represented among them (see Supplemental Figure 1 online), the most common ones having either a transversion or a deletion of one of the TSD central bases, as has been observed in other *Ac* or *Ds* mutable alleles (Kunze and Weil, 2002). Overall, simple *Ac* excisions (Bz′) are 21 times more frequent than the more complex *Ac* mutations (bz-s). Both types of exceptions occur twofold to threefold more frequently in the male than in the female germline. However, the types of mutation generated from *bz-m39*(*Ac*) males or females do not seem to differ (see below and in Supplemental Figure 1 online).

Characterization of bz-s Derivatives from *bz-m39*(*Ac*)

Three diagnostic PCRs were performed on all bz-s derivatives. As shown in Figure 2A, primer pair *a*+*b* amplifies the 5′ *Ac-bz* junction, primer pair *c*+*d* amplifies the 3′ *Ac-bz* junction, and

Figure 1. *bz-m39*(*Ac*) Phenotypes.

Unstable kernel, plant, and anther phenotype of progeny from a cross between *bz-m39*(*Ac*) as male and *sh-bz-X2* as female. The bronze kernel carries a bz-s mutation.

Table 1. Frequencies of bz-s and Bz′ Derivatives from *bz-m39*(*Ac*) Female and Male Parents

Cross	Type of Derivative	Effective Population	No. of Selections	Frequency ($\times 10^{-3}$)	Bz′: bz-s	Male: Female
Sh bz-m39(*Ac*) *wx* x *sh-bz-X2 wx*	bz-s	5690	11	1.9	27.8	2.7
sh-bz-X2 wx	Bz′	466	25	53.6		1.8
sh-bz-X2 wx x *Sh bz-m39*(*Ac*) *wx*	bz-s	11870	61	5.1	18.8	
sh-bz-X2 wx	Bz′	550	53	96.4		

primer pair *a*+*d* amplifies the entire transposon plus the adjacent *bz* sequences in long-range PCR. The bz-s derivatives were then grouped into six categories according to the PCR results (Figure 2B). The parental *bz-m39*(*Ac*) allele produces junction PCR products with the *a*+*b* and *c*+*d* primer pairs and two PCR products with the *a*+*d* primer pair: a large one, corresponding to the *Ac*-occupied site, and a 4.5-kb smaller one, corresponding to the *Ac* excision or empty site. The derivatives producing nonparental PCR patterns were tentatively classified as follows. Derivatives producing the same two PCR products with the junction primers, but no empty site and a smaller band than the *Ac*-occupied site with the *a*+*d* primer pair, were classified as new *Ds* elements. Derivatives producing only one of the two junction products were classified as *fAc* elements or *Ac*-adjacent deletions. Derivatives that failed to amplify either junction, but yielded a product with the *a* and *d* primers were classed as adjacent deletions without *Ac*.

The *a*+*d* PCR products from putative *Ds* elements (class 2) were digested separately with the *Ac*-cutting enzymes *Pvu*II, *Hind*III, and *Eco*RI to identify the deleted region, and deletion junctions were then sequenced. The PCR products from the lines that have undergone an *Ac* excision and an adjacent deletion were small, so the whole PCR fragments were sequenced directly. To obtain the junction sequences of the *fAc*s and the *Ac*-adjacent deletions, sequential PCRs were performed using combinations of an *Ac*-specific primer and a series of primers based on the adjacent *stk1* and *stc1* genes and the intergenic regions (not shown in Figure 2A). Alternatively, inverse PCR was used to solve larger genomic alterations involving *fAc* or *Ac*-adjacent deletions. Sequencing of the PCR products identified the novel junctions.

In addition, the bz-s derivatives were subjected to a series of genetic tests. They were self-pollinated to confirm heritability of the selected bz-s phenotype and crossed to *bz-R wx-m7*(*Ac*) to determine whether a *Ds* element resided at *bz*. All non-*Ds* derivatives and derivatives with small internal deletions were crossed to *bz-m2*(*D1*) to determine whether they retained *Ac* activity.

Ds Formation

A total of 54 internal deletions were identified among the 72 bz-s selections. All but two of them behaved as *Ds* elements when crossed to *bz-R wx-m7*(*Ac*). They retain mutability in the presence of *Ac*; therefore, the new mutable alleles are designated *bz-m39.x* to indicate that they are *Ds* derivatives of *bz-m39*(*Ac*). Six of them apparently arose from three premeiotic events, bringing the number of unique *Ds* elements to 49. Correcting for these duplicate events, the minimal mutation frequencies of *Ac* to *Ds* are 0.9×10^{-3} and 3.7×10^{-3} in female and male gametes, respectively (mutations in which *Ac* is retained in the genome are not selected). The new *Ds* elements range in size from 1.1 to 4.6 kb (Figure 3). Although the internal deletions do not seem to occur at any specific location, as seen in previous studies (Yan et al., 1999; Conrad et al., 2007), most *Ds* deletions extended into the central 2.2- to 3.2-kb segment of *Ac*, revealing a preferential region for deletion formation. In response to *Ac*, most internal deletions can excise at a similar frequency as the parental *Ac39*, with a few exceptions. *bz-m39.31* retains just 119 bp of the 5′ end and produces few very fine spots when crossed to *Ac*, so this deletion of *Ac* corresponds to a new *Ds* element with minimal transposition activity (see Supplemental Figure 2 online). The element in *bz-s39.48* has only 66 bp left of the 5′ end, and a cross to an *Ac* source (*wx-m7*) resulted in only stable bronze kernels, indicating that this element is not a bona fide *Ds*.

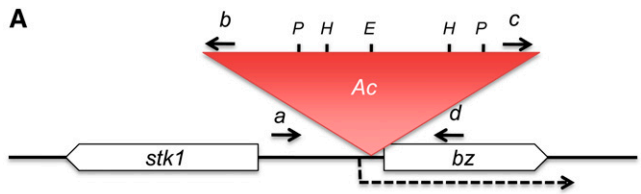

B

	Classes of mutations	*a*+*b*	*c*+*d*	*a*+*d*
1	*Ac*	+	+	+(2)
2	*Ds*	+	+	+
3	*fAc*, 5′ end retained	+	-	+/-
4	*fAc*, 3′ end retained	-	+	+/-
5	Adjacent deletion, Ac retained	+/-	-/+	-
6	Adjacent deletion, Ac lost	-	-	+/-

Figure 2. PCR Characterization of bz Derivatives.

(A) Structure of *bz-m39*(*Ac*), showing *Ac* inserted in the 5′ UTR of the *bz* gene. The *bz* transcript is represented by the dotted arrow; *Ac* and *bz* are in the same transcriptional orientation. Primers and their approximate locations are indicated by short arrows. Primers *a* and *d* anneal to sequences adjacent to *Ac39*; primers *b* and *c* anneal to the *Ac* subterminal region. E, *Eco*RI restriction site; H, *Hind*III restriction site; P, *Pvu*II restriction site.

(B) Summary of the PCR amplification patterns given by the various derivatives. The derivatives fell into six classes based on the PCR results. +, band present; −, band absent; +/−, band present in some derivatives, absent in others; +(2), two bands amplified.

[See online article for color version of this figure.]

The phenotypes of both *bz-m39.31* and *bz-s39.48* agree with earlier findings in transgenic tobacco (*Nicotiana tabacum*), in which transposons retaining between 100 and 200 bp of one end had reduced excision frequencies, whereas those retaining less than 100 bp at either end showed no excision (Coupland et al., 1989). *bz-m39.55* is the largest *Ds* element found in this study. It has a 3-bp in-frame deletion in the second exon that results in the loss of Ser-305, a well-conserved residue within the *Ac*/*Tam3* and *restless* clades of *hAT* DNA transposases (see Supplemental Figures 3A and 3B online) that is evidently important for activity. Finally, *bz-s39.24* has a tiny deletion close to the 5′ end and behaves like an immobile *Ac* (discussed later).

Most *Ds* deletion junctions occur at short (2- to 9-bp) sequences that are internally duplicated in *Ac* (Figure 4). Filler DNA is commonly found at the junctions of genetic rearrangements (Roth and Wilson, 1985; Roth et al., 1989; Sainsard-Chanet and Begel, 1990; Wessler et al., 1990) and of approximately one-half of previously characterized *Ds* elements (Yan et al., 1999; Conrad et al., 2007). Seventeen out of 49 (35%) newly formed *Ds39* elements have filler DNA between the deletion endpoints. The size of the filler from this study varies from 2 bp in *Ds39.35* to 55 bp in *Ds39.63* (Figure 5). In most cases, the filler DNA sequences also appear close to deletion termini in the progenitor *Ac* sequence, where they are flanked by microhomologies to the *Ds* sequences flanking the filler DNA (shown in bold in Figure 5). Interestingly, most of the *Ds* elements with filler DNA (16 of 17) display microhomology at each junction. The filler DNA from eight *bz-s39* derivatives originated from more than one location. For example, *Ds39.87* has a 32-bp filler derived from three locations within *Ac*, namely 8 bp from 3799 to 3806, 10 bp from 2036 to 2045, and 14 bp from 2008 to 2021, and all three pieces of filler DNA share microhomology with each other at the junctions.

fAc

Nine single-ended or *fAc*s occurred in the collection of stable bronze derivatives, of which six retain the 3′ end of *Ac*, whereas three retain the 5′ end. The complete structure of seven of them is shown in Figure 6, but two of them had complex rearrangements at the fractured end whose detailed structure could not be elucidated. The size of the *fAc* elements ranges from 0.5 to 4.5 kb. In every *fAc*, the terminal *Ac* deletion is accompanied by changes in the sequence adjacent to *Ac* in the *bz-m39*(*Ac*) progenitor allele. Two types of *fAc* derivatives were recovered. One type comprises *bz-s39.42*, *bz-s39.57*, *bz-s39.77*, and *bz-s39.88*. In these four alleles, the 3′ (right) *Ac-bz* junction is identical to that in the parental allele, but the 5′ (left) side is complex. The 5′ end of *Ac* has been deleted, leaving a 3′ *fAc* ranging in size from 0.5 to 2.4 kb. Immediately 5′ of the *fAc*, a 4- to 62-bp duplication of *bz* sequences adjacent to the *Ac* 3′ junction ends in a canonical *Ac39* excision footprint. The other type of *fAc* derivative comprises *bz-s39.86*, *bz-s39.37*, and *bz-s39.94*. These alleles also have one parental *Ac-bz* junction, but an adjacent deletion, rather than duplication, of *bz* sequences accompanies the *Ac* terminal deletion. *bz-s39.86* has an intact right *Ac-bz* junction, but is missing 18 bp from the 5′ *Ac* end and 738 bp of adjacent upstream *bz* sequence. *bz-s39.37* has an intact left *Ac-bz* junction, but is missing 2591 bp from the 3′ *Ac* end and 2877 bp of adjacent downstream *bz* sequence. Similarly, *bz-s39.94* has an intact left *Ac-bz* junction, but is missing 385 bp from the 3′ *Ac* end and 2118 bp of adjacent downstream *bz* sequence. The deletion junctions in all *fAc* elements occur at sites of direct repeats of a few bases in the *bz-m39*(*Ac*) parental allele (Figure 7). Three of these junctions have short filler DNAs with similar properties to those found in *Ds* deletion junctions.

Adjacent Deletions with and without Retention of *Ac*

Seven stable *bz* alleles had deletions of gene sequences adjacent to *Ac* (Figure 8). The deletions range in size from 52 to 7011 bp and can occur at either end of *Ac*, often extending into either the proximal *stk1* or distal *stc1* gene. Five have intact *Ac* and *bz* sequences at one end and precise deletions of gene sequences at the other. In this sample, three were next to the 5′ end (*bz-s39.26*, *bz-s39.29*, and *bz-s39.38*), whereas two were next to the 3′ end (*bz-s39.22* and *bz-s39.43*). On subsequent excision of *Ac*, the former three would result in fusions of a promoterless *bz* gene to different fragments of the proximal *stk1* gene in opposite orientation. The latter two would result in fusions of the *bz* promoter to different fragments of the distal *stc1* gene in opposite orientation, an arrangement that could lead to the formation of antisense RNA. In the remaining two adjacent deletions, *bz-s39.66* and *bz-s39.81*, *Ac* has also excised, leaving behind one-half of typical excision footprints at *bz*: a transversion and a deletion of the base nearest *Ac*, respectively. These deletions are small (185 and 52 bp), but removal of the *bz* promoter and of part of the coding sequence, respectively, leads to a null *bz* phenotype.

Immobilized *Ac*

bz-s39.24 is a stable bronze mutation that behaved like a *Ds* derivative in the three diagnostic PCR tests designed to identify structural changes in *Ac39* (Figure 2) but did not respond to *Ac* in genetic crosses to *wx-m7*(*Ac*). Surprisingly, the lack of mobility of *bz-s39.24* results from a tiny, 7-bp deletion of nucleotides 22 to 28 in the 5′ subterminal region (Figure 3). The immobilized *Ac* (*Ac-im*) element described by Conrad and Brutnell (2005) lacks 10 bp from the 5′ TIR, which was known to be essential for excision (Hehl and Baker, 1989; Kunze and Weil, 2002). The 7-bp deletion in the 5′ subterminal region of *bz-s39.24* leads to a similar immobility, revealing a new *cis* requirement for *Ac* transposition. The immobile 4558-bp element retains full *Ac* transposase activity and can transactivate excision of the *Ds* element in the *bz-m2*(*Dl*) reporter as well as the intact *Ac* element in *wx-m7*(*Ac*); therefore, we have called it *Ac-im2*.

bz-s39.86 is a single-ended *fAc* derivative that has lost the 5′ terminal 18 bp of *Ac* and 738 bp of adjacent *bz* sequence (Figure 6). In agreement with previous findings (Hehl and Baker, 1989; Xiao and Peterson, 2002; Conrad and Brutnell, 2005), the small terminal deletion completely eliminated the ability of *Ac* to transpose. The *fAc* element in *bz-s39.86* is similar to *Ac-im* (Conrad and Brutnell, 2005), having lost an additional 8 bp from the 5′ end, and like *Ac-im* and *Ac-im2*, it can also transactivate

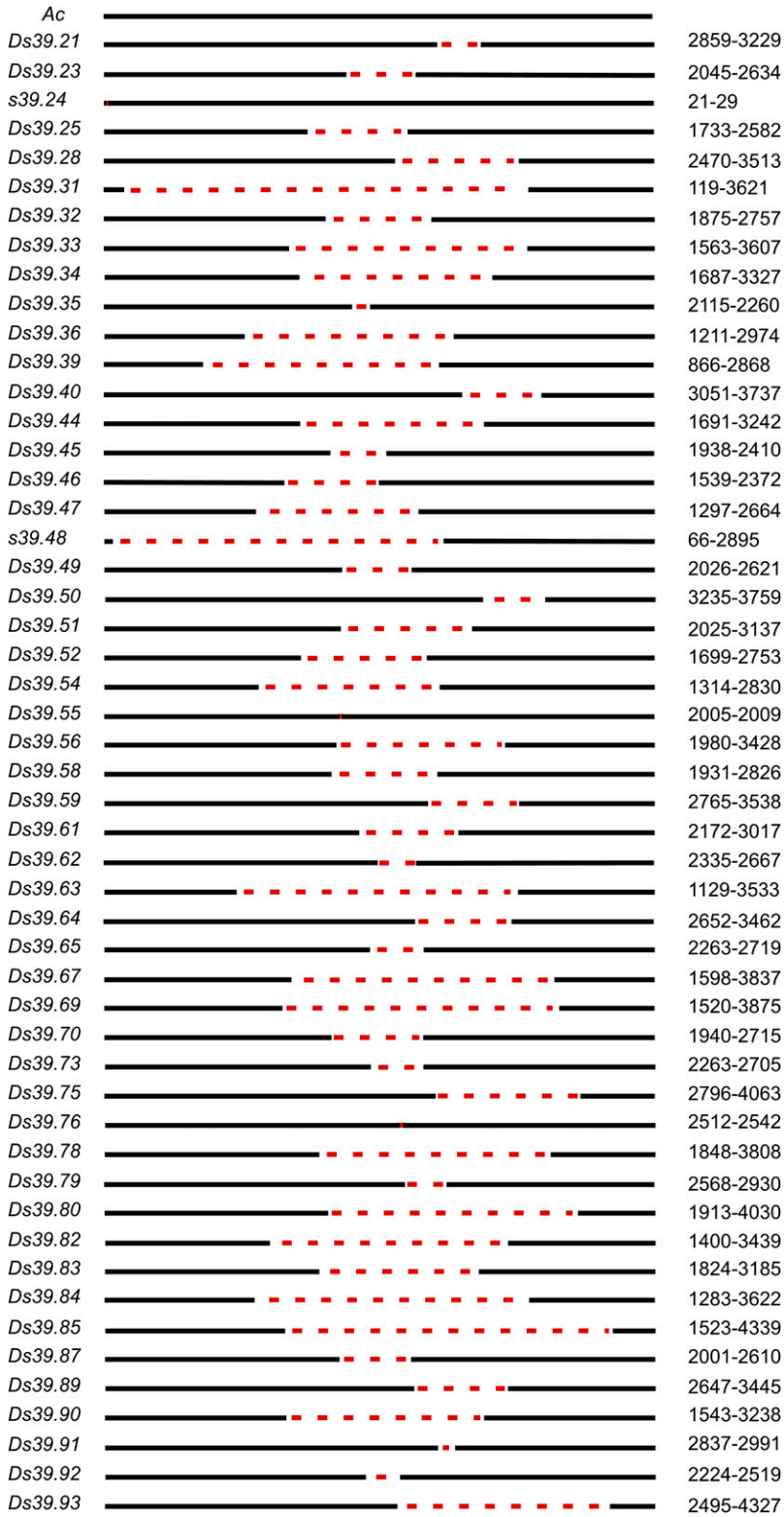

Figure 3. Structure of 51 Internal Deletions from *Ac39*.

Solid lines indicate *Ac* sequences, and dotted line represent deletions. All but *bz-s39.24* and *bz-s39.48* are true *Ds* elements. Short filler DNAs are not shown in the figure, but their sequences can be found in Figure 4.
[See online article for color version of this figure.]

	Left junction	Right junction
Ac	TGAGTGAAAA GTTTGAGAAA	TTGATATTTT ATCATGGTGG
bz-s39.21	TGAGTGAAAA	ATCATGGTGG
Ac	CCATCC**ATTG** GATTGATGA	TCAATT**ATTG** TAGGTACGAT
bz-s39.23	CCATCC**ATTG**	TAGGTACGAT
Ac	TCATGG**CAAA** GACATAAATC	TTTGTCT**CAA** TTGTTGTACA
bz-s39.25	TCATGG**CAAA**	TTGTTGTACA
Ac	ATATGA**TGTC** TCAACTAGAT	TATTTG**TGTC** ATTCAAGGTG
bz-s39.28	ATATGA**TGTC**	ATTCAAGGTG
Ac	CCCTCAC**TTT** CCAATAAAGT	CTGCAAA**TTT** ATTTTACAAA
bz-s39.32	CCCTCAC**TTT**	ATTTTACAAA
Ac	GGTCG**ATGGA** AAGAAATACG	ATCAT**ATGGA** TGAGGTATTT
bz-s39.33	GGTCG**ATGGA**	TGAGGTATTT
Ac	GTTT**ATAACA** GGGTTGAAAA	GATTC**ATACA** AAGTTCATGT
bz-s39.36	GTTT**ATAACA**	AAGTTCATGT
Ac	GTCCTT**CAGC** TCCAAAGACA	GCTGCC**CAGC** CGTGTTATAC
bz-s39.40	GTCCTT**CAGC**	CGTGTTATAC
Ac	AGAAA**AAGAA** AAGTTGTATG	GTGGG**AAGAA** CTAATGAAGT
bz-s39.45	AGAAA**AAGAA**	CTAATGAAGT
Ac	GATGTG**GCCG** CACATCACCA	CCTAAA**GCCG** AGGAGTGGAA
bz-s39.47	GATGTG**GCCG**	AGGAGTGGAA
Ac	GTTAGTTT**TA** TCCCGATCGA	TATTGCAC**TA** GCTGTAGCAT
bz-s39.48	GTTAGTTT**TA**	GCTGTAGCAT
Ac	AAGTCATA**CA** TGTGTGTCAC	CAATTAAT**CA** AATGTCAATT
bz-s39.49	AAGTCATA**CA**	AATGTCAATT
Ac	TCATGG**TGGA** GGGGAAGGGT	ATGGC**TGGCA** TTAACAGATT
bz-s39.50	TCATGG**TGGA**	TTAACAGATT
Ac	CCATCA**TCAT** CAACAGCTGA	AATTTG**TCAT** TAGGAGAATG
bz-s39.54	CCATCA**TCAT**	TAGGAGAATG
Ac	ATATGTGGAC ATCTTGTCAA	TGTGGACATC TTGTCAAAAT
bz-s39.55	ATATGTGGAC	TTGTCAAAAT
Ac	CTCGCTTC**AG** TACAACTATG	CAGCATCT**AG** AAAAGGTGAA
bz-s39.56	CTCGCTTC**AG**	AAAAGGTGAA
Ac	TTTGT**ATTTG** GAAGAAAAAG	GAAAA**ATTTG** TCATTAGGAG
bz-s39.58	TTTGT**ATTTG**	TCATTAGGAG
Ac	AATT**TATTTT** A**CAA**AGGTTT	TACA**TATTTT** C**CAA**CAATGA
bz-s39.59	AATT**TATTTT**	C**CAA**CAATGA
Ac	AA**CATTGAGAAAA** AA**TTGT**TTGC	GGT**CATTAGAAAA** **TTGT**ATCAAT
bz-s39.61	AA**CATTGAGAAAA**	TTGTATCAAT
Ac	AGGATGGCTT **GG**CTGTAATT	CTAAAGCCGA **GG**AGTGGAAG
bz-s39.62	AGGATGGCTT	**GG**AGTGGAAG
Ac	CAATTTG**TCC** TAAAGCCGAG	ATGAAGT**TCC** AATTTATAGT
bz-s39.64	CAATTTG**TCC**	AATTTATAGT
Ac	ATTCAA**ATCT** AGTTTGTGAT	TTTTTG**ATCT** CACTGAACTC
bz-s39.65	ATTCAA**ATCT**	CACTGAACTC
Ac	CACATCGGAT GTATGGCAGC	GCTGCCTAGC TCCCAGCCGT
bz-s39.69	CACATCGGAT	TCCCAGCCGT
Ac	AATCT**AGTTT** G**TGAT**GGTGC	GAAGA**AGTTT** TT**TGAT**CTCA
bz-s39.73	AATCT**AGTTT**	TT**TGAT**CTCA
Ac	ATTTGAT**TGA** C**CAATG**GTGT	CTCTCCA**TGA** G**CAATG**TGTC
bz-s39.75	ATTTGAT**TGA**	G**CAATG**TGTC
Ac	TTGAGGGATG C**CTTA**TATTA	CACTAATAAG G**CTTA**AAACA
bz-s39.76	TTGAGGGATG	G**CTTA**AAACA
Ac	TTG**TTGAGTT** TGTTAAGTCT	TGTT**TTGATT** GGCTGCTAGC
bz-s39.78	TTG**TTGAGTT**	GGCTGCTAGC
Ac	AGATGAT**ATG** GCTATTGTTC	AAGGTGA**ATG** CATATATGTT
bz-s39.82	AGATGAT**ATG**	CATATATGTT
Ac	CTTTC**AATAT** **TGT**AGAACAT	GGATA**AATAT** **ATGT**CTGAAC
bz-s39.83	CTTTC**AATAT**	**ATGT**CTGAAC
Ac	ACGATGCA**AT** **TTGT**CCTAAA	GAATGCAT**AT** **ATGT**TATAAT
bz-s39.89	ACGATGCA**AT**	**ATGT**TATAAT
Ac	CATTAGG**AGA** ATGGCCGTTG	TTCATGT**AGA** TGACTTTGTT
bz-s39.91	CATTAGG**AGA**	TGACTTTGTT
Ac	TGCACG**ATAT** AATTGAGGAT	TGCCTT**ATAT** TATAAGCCTG
bz-s39.92	TGCACG**ATAT**	TATAAGCCTG
Ac	AACC**TATTTG** ATGTTGAGGG	TTTA**TATTTG** TTTTTAAGTT
bz-s39.93	AACC**TATTTG**	TTTTTAAGTT

Figure 4. Sequence of the *Ds* Deletion Junctions.

Sequences of the left (5′) and right (3′) deletion junctions and the corresponding sequence in *Ac* are shown for each *Ds* element. Microhomology sequences are shown in boldface.

excision of *Ds* from a reporter allele. We have termed this 4547-bp element *Ac-im3*.

Methylated *Ac*

bz-c39.27 was selected as a stable bronze mutation and behaved like a *Ds* derivative in the PCR assay (category 2 in Figure 2B). However, sequencing of the entire element revealed no changes at the nucleotide level. After two generations of selfing, this allele regained a weak *Ac* transposase activity. Crosses to *bz-m2*(*DI*) produced many very fine spotted kernels together with a few heavy spotted kernels, and a somatic excision product could be detected by PCR with primers *a* and *d* that was absent in the previous generation (see Supplemental Figure 4A, i, online). PCR assays indicated that the internal *Pvu*II sites of *Ac* were methylated in the first two generations but were hypomethylated in the third (see Supplemental Figures 4A, ii and iii, online), and a DNA gel blot confirmed that the *Pvu*II sites were unmethylated on reactivation (see Supplemental Figure 4B online). Thus, like other *Ac*s (Schwartz and Dennis, 1986; Chomet et al., 1987; Brutnell and Dellaporta, 1994), *Ac39* can undergo cycles of activity that correlate with its methylation state. Although this derivative was originally labeled *bz-s*, because of its stable bronze phenotype, we have renamed it post facto as *bz-c39.27* to indicate its cycling nature.

Retrotransposon Insertion Mutation

bz-s39.71 is a most unusual derivative. It has an intact *Ac* at the original insertion site of *bz-m39*, but it heritably produces stable *bz* kernels. Further analysis revealed that the loss of instability was not related to an *Ac*-induced change but to the chance insertion of a *Magellan* LTR retrotransposon 65 bp upstream of the *Ac* insertion site. The retrotransposon insertion not only stabilizes *bz* but also interferes with *Ac* function, as evidenced in a cross with a *bz-m2*(*DI*) tester that produced very few purple spots.

DISCUSSION

Frequencies of *Ac* Mutation

On transposition, TEs cause mutations not only of host genes but of themselves. However, because most TEs are followed phenotypically by their effect on host genes, their mutations are detected only indirectly as changes in the mutable phenotypes produced by the host genes into which they are inserted. In mutable alleles where *Ac* is inserted within the coding sequence, loss-of-instability mutations of *Ac* usually have the same phenotype as the much more numerous *Ac* simple excision footprints. Among those mutations, *Ds* elements originating de novo can be identified, because their stable phenotype is reversible; therefore, putative mutations of *Ac* to *Ds* can be established by a series of rather tedious genetic tests. Estimates of *Ds* mutation frequencies in the literature are scant. McClintock (1963) isolated two *Ds* derivatives from a combined total of 4700 *wx-m9* (*Ac*) male and female gametes produced in *Ac*/+ heterozygotes. Therefore, the *Ac* to *Ds* mutation frequency from this small

	Left junction	Filler	Right junction
Ac	110-ACGG**AAACGG** GATATA		GGTATT **TA**AAGATTAT-3630
Ds39.31	ACGG**AAACGG**	---aaacggaaag---	**TA**AAGATTAT
filler origin		1-CAGGGATGAAAGTAGGATGGGA-22	
		131-CGGT**AAACGG**AAACG**GAAA**CGGTAGA-156	
Ac	1678-CACATAG**TTT** AGTTAA		AGTCTG C**GTT**CAGTGC-3336
Ds39.34	CACATAG**TTT**	---cgaaatcacata---	C**GTT**CAGTGC
filler origin		1648-CAAGCGGA**TTT**CGAA**ATCAC**TTGAGAAC**ATCAC**ATA**GTT**TAGTTAAAGG-1696	
Ac	2106-CGCCAC**ACTG** GCCAAA		TCAAAT **CT**AGTTTGTG-2271
Ds39.35	CGCCAC**ACTG**	---aa---	**CT**AGTTTGTG
filler origin		2303-TCACAT**ACTG**AA**CT**TGGTTGCA-2324	
Ac	857-CTGC**TGATTG** CTGTCC		TTGAGA **AATAT**TGGAA-2877
Ds39.39	CTGC**TGATTG**	---agttct---	**AATAT**TGGAA
filler origin		2933-ATAT**TGATTG**AGTTCT**ATAT**GAAAAAA-2959	
Ac	1682-TAGTTTA**GTT** AAAGGT		TGGAGG GGAAGGGTTG-3251
Ds39.44	TAGTTTA**GTT**	---gcagaatatcaacgc---	GGAAGGGTTG
filler origin		3241-GGGAAGG**GTT**GCAGAATATCCTATTCTCAC-3270. AACGC: two locations in Ac	
Ac	1530-CATTT**CACCA** AGAAGG		CAAAGC **GA**TTGTTCTT-2381
Ds39.46	CATTT**CACCA**	--- cagaa---	**GA**TTGTTCTT
filler origin		1481-AGAAG**CACCA**CAGAA**GA**GGGCAAAG-1505	
Ac	2016-AATAAGTC**AT** ACATGT		TTGCAT **GAG**TTGAAGG-3146
Ds39.51	AATAAGTC**AT**	---gatcaagta---	**GAG**TTGAAGG
filler origin		3142-GAAGGATT**AT**GATCAAGTA**GAG**TCAAATG-3170	
Ac	1690-TTAAA**GGTCA** GTTGTG		TCCACT **GC**AAATTTAT-2762
Ds39.52	TTAAA**GGTCA**	---tcatggaacaa---	**GC**AAATTTAT
filler origin		1630-CTGAG**GGTCA**TCATGGAACAA**GC**GGATTTCG-1660	
Ac	1120-TAGAAAAA**CA** GTAGCA		CTACAT **ATT**TTCCAAC-3542
Ds39.63	TAGAAAAA**CA**	---aattccggttggaaataatcctccctcaggctcagccataagattggccaagttg---	**ATT**TTCCAAC
filler origin		1074-TCGCAAAA**CA**AATTCCGTATTCTC-1097	
		993-GCC**TCC**GGTTGGAAATAATCCTCCCTCAGGCTCAGCCATAAGATTGGCCAAGTTG**AT**GTC-1052	
Ac	1589-GGGACAT**TGC** AACTTT		TGTTAG **GCTCCCAGC**T-3846
Ds39.67	GGGACAT**TGC**	---cta---	**GCTCCCAGC**T
filler origin		3860-TGCTAGC**TGC**CTA**GCTCCCAGC**C-3882	
Ac	1931-GGAAGA**AAAA** GAAAAG		TTTTTG **ATC**TCACTGA-2724
Ds39.70	GGAAGA**AAAA**	---tat---	**ATC**TCACTGA
filler origin		1901-TGCTAG**AAAA**TAT**ATC**ATGGATT-1923	
Ac	2559-CCTCGCAG**GT** ATGTTT		TACAAG **AAAA**TATTGA-2939
Ds39.79	CCTCGCAG**GT**	tagggtcattagaaaaaatattgattcaacctatttaaataaggctt---	**AAAA**TATTGA
filler origin		2991-ATGACTTT**GT**TAGGGTCATTAG**AAAA**TTGTATCAAT-6026	
		2924-TACAAG**AAAA**TATTG**ATT**GAGTTCTATA-2951	
		2481-AGATGGA**ATT**CAACCTATTTGATGTTGAGG-2510	
		3612-TGAGGTA**TT**TAAAGATTATTAT-3633	
		3529-CCTGCACT**AA**TAAGGCTT**AAAA**CAAGTG-3556	
Ac	1904-TAGAA**AATAT** ATCATG		TCTAAG **AATA**ATGAAG-4039
Ds39.80	TAGAA**AATAT**	---cctttc---	**AATA**ATGAAG
filler origin		1808-GCATG**AATAT**CCTTTC**AATA**TTGTAG-1833	
Ac	1283-GCATGGA**TGT** GGCCGC		GTATTT **AAA**GATTATT-3631
Ds39.84	GCATGGA**TGT**	---ttatacgaaaaatctgtttat---	**AAA**GATTATT
filler origin		1200-AAAAATC**TGT**TT**ATA**ACAGGGT-1221	
		1188-TAGAATA**ATA**CGAAAAATCTGTTTAT**AA**CAGGGT-1221	
Ac	1514-ATCGGAT**GTA** TGGCAG		TTTTTA **AG**TTTTGAAT-4348
Ds39.85	ATCGGAT**GTA**	---atgcaaagaagtgg---	**AG**TTTTGAAT
filler origin		1353-AGCAGTA**GTA**ATGC**AAA**TGGTACAGCT-1379	
		1771-TGGTTAGCCT**AAAGAAG**CTTCATTTGG-1797	
		1542-AAGGAAATT**GAAG**TGG**AG**GTCGATGG-1567	
Ac	1992-ATGGATA**TGT** GGACAT		AAATTC **TCA**ATTAATC-2619
Ds39.87	ATGGATA**TGT**	---cgccttgtcaccatccattgtcaaaataag---	**TCA**ATTAATC
filler origin		3789-TGCGCCT**TGT**CGCCT**TGT**TTTGATT-3813	
		1998-ATGTGGA**CAT**CTTGTCAAAATAAG**TCA**TACATGTGT**TGT**CACCATC**CAT**TGGATTG-2052	
Ac	1530-CATTTCAC**CA** AGAAGG		ATGGTG **GAGGG**GAAGG-3247
Ds39.90	CATTTCAC**CA**	---gaa---	**GAGGG**GAAGG
filler origin		1483-AAGCACCA**CA**GAA**GAGGG**CAAAG-1505	

Figure 5. Sequences of the *Ds* Filler Junctions.

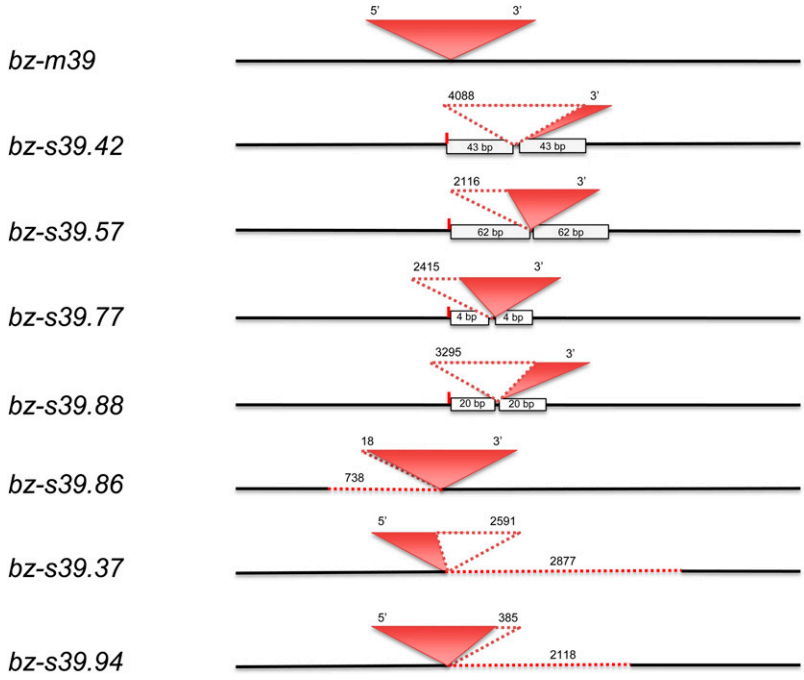

Figure 6. Structure of *fAc*s.

Boxes represent duplicated *bz* sequences, dotted lines represent deletions, and their sizes (in bp) are shown above each rearrangement. Short vertical lines denote excision footprints at the original insertion site of *Ac*. All alleles are aligned at this site.
[See online article for color version of this figure.]

experiment would be 4×10^{-4}. A caveat here is that, although the male and female gamete populations were reported separately, the actual source of the two mutations was not identified, so the above frequencies represent combined estimates from the two sexes. Yan et al. (1999) obtained two *bz-m2*(*Ds*) derivatives from 3867 *bz-m2*(*Ac*) gametes produced in *Ac*/+ heterozygous females, for a frequency of 5×10^{-4}. Conrad et al. (2007) isolated five new *Ds* elements from four different loci out of a total population of 19,923 gametes produced in *Ac*/*Ac* homozygous females, for an average frequency estimate of 2.5×10^{-4}. The one conclusion that can be drawn from the above is that the frequency with which *Ac* mutates to *Ds* from one generation to another is on the order of 10^{-4}, but whether the mutation frequency varies from locus to locus, within a locus, or between sexes is unclear. Other loss-of-instability mutations of *Ac* can only be sorted out from the much more numerous excision footprints by molecular tests, so neither their types nor frequencies have been well documented to date.

Here we report a high frequency of *Ac* mutations at the *bz-m39*(*Ac*) allele, including a much higher frequency of mutation to *Ds* than reported previously: 0.9×10^{-3} on the female side and 3.7×10^{-3} on the male side. These two frequencies differ very significantly from each other ($\chi^2 = 11.1$, 1 *df*, $P < 0.001$), indicating that *Ac* mutates more frequently in the male than in the female germline. The same is true for *Ac* excisions, which are 1.8 times more abundant in the male (9.6%) than in the female (5.4%). However, the types of mutation generated in the two sexes do not seem to differ.

The *bz-m2*(*Ac*) and *bz-m39*(*Ac*) alleles arose in the same *Bz-McC* haplotype (Fu et al., 2001), providing us with the opportunity to compare the frequency of *Ac* excision from two different locations of the same *Bz* allele and in the same genetic background. *Ac* is inserted in the 5′ UTR in *bz-m39*(*Ac*) versus the second exon in *bz-m2*(*Ac*) (Fedoroff et al., 1984). *Ac* excision from both alleles generates Bz′ and bz-s derivatives, although the Bz′:bz-s ratio in *bz-m2*(*Ac*) is much lower (0.48), because most *Ac* excisions fail to restore gene function. The combined frequency of Bz′ and bz-s derivatives from *bz-m2*(*Ac*)/*bz* heterozygous female parents in an experiment involving 5650 *bz-m2* gametes was 2.1% (Dooner and

Figure 5. (continued).

Sequences of the left (5′) and right (3′) deletion junctions and the corresponding sequence in *Ac* are shown for each *Ds* element. Microhomology sequences are bolded. Filler DNA is shown in lowercase, and the *Ac* sequence from which it originated is shown in underlined uppercase. Numbers refer to coordinates in the *Ac* sequence (GenBank X05425). Colored filler sequences denote multiple origins in the *Ac* sequence, where they are represented in the same color.

	Left junction	Filler	Right junction
m39	115079-GGCGCCC**GCC** GACGGC		TTGTTG **ACAG**ATGAGC
bz-s39.42	GGCGCCC**GCC**	---tagccga---	**ACAG**ATGAGC
filler origin	115043-GCGGCTA**GCC**TAGCCGA**ACAG**CCTGAG-115067		
footprint	CTAGCGGG/-TAGCGGC		
m39	AGTCCTCCCC **GCC**GCC		ACACTG **GCC**AAAGGTT
bz-s39.57	AGTCCTCCCC		**GCC**AAAGGTT
footprint	CTAGCGGGC/--AGCGGC		
m39	AGCGGCTAGC **CTA**GCC		GAAGAA **CTA**ATGAAGT
bz-s39.77	AGCGGCTAGC		**CTA**ATGAAGT
footprint	CTAGCGGG/-TAGCGGC		
m39	GAACAGCCTG **AGC**GCG		TGTGCT **AGC**AATACAA
bz-s39.88	GAACAGCCTG		**AGC**AATACAA
footprint	CTAGCGGGC/--AGCGGC		
m39	TTATATACAGA **AT**TGTG		AGTAGG **AT**GGGAAAAT
bz-s39.86	TTATATACAGA		**AT**GGGAAAAT
m39	GATGTTCA**GT** CTCGCT		CCTCTC **AAGTG**CCTCA-117924
bz-s39.37	GATGTTCA**GT**	---acg---	**AAGTG**CCTCA
filler origin	118121-AGCCTGCC**GT**ACG**AAGTG**AACAC-118143		
m39	ACTTTATA**TT** GTGTCA		CCGAAC **TG**AGGAACCG-117171
bz-s39.94	ACTTTATA**TT**	---atg---	**TG**AGGAACCG
filler origin	127176-TTTGTGGT**TT**ATG**TG**GAGATCTA-127198		

Figure 7. Sequence of Excision Footprints and Deletion Junctions of *fAc* Elements.

Sequences of the left (5′) and right (3′) deletion junctions and the corresponding sequence in *Ac* are shown for each *fAc* element. Microhomology sequences are shown in boldface. Filler is shown in lowercase. The numbers identify the nucleotide positions of the filler DNA origins relative to the sequence of the 226-kb McC *bz* haplotype contig.

Belachew, 1989), less than one-half of that from *bz-m39*(*Ac*)/*bz* heterozygotes in a similar sized experiment (Table 1). The difference between these two frequencies is highly significant (χ^2 = 73; 1 *df*; P < 0.001), indicating that the location of *Ac* within the gene affects its transposition frequency. Most likely, the proximity to the *bz* promoter accounts for the enhanced transposition of *Ac39*.

Estimates of spontaneous mutation frequencies in different organisms range from 10^{-5} to 10^{-6}, 1000-fold lower than the *Ac* mutation frequency, suggesting that the DSBs caused by *Ac* transpositions play an important role in the formation of the mutations. Furthermore, in somatic tissues of transgenic tobacco, only *Ac*, but not a nearly identical *Ds* element, is capable of generating internal deletions, indicating that their formation is transposition-dependent (Rubin and Levy, 1997). In the mechanisms for the formation of different *Ac* mutations proposed below, all *Ac* mutations are accompanied by transposition events. DNA ends produced by *Ac* excision are often ligated without the need for homology (NHEJ pathway). More rarely, they are repaired via an error-prone DNA synthesis pathway (Yan et al., 1999) that shares features with a synthesis-dependent microhomology-mediated end joining (MMEJ) pathway recently proposed to explain DSB repair in *Drosophila* (Yu and McVey, 2010).

Models for *Ac* Mutations

Nearly all (70 of 72) stable bz derivatives from *bz-m39*(*Ac*) can be grouped into one of two general categories: either with or without rearrangements of transposon sequences. The former include internal and terminal deletions of *Ac* and constitute formal mutations of *Ac*. The most frequent mutations of *Ac* are internal deletions, most of which behave as *Ds* elements. More than two-thirds (68.5%) of *Ac* mutations fall under this category. Out of the 49 newly formed *Ds* elements, 45 (90%) have 2- to 9-bp microhomologies at the deletion junction, suggesting an origin by a mechanism involving strand invasion and synthesis from both ends, followed by MMEJ and, therefore, deletion of the sequence between the two sites (Figure 4). As illustrated in Figure 9A, repair of the DSB caused by *Ac* excision would be initiated by strand invasion from both ends to begin copying the *Ac* sequence in the sister chromatid. MMEJ between two short direct repeats (GTC in the example in Figure 9A) results in the deletion of one repeat and the sequence between the two repeats, yielding a new *Ds* element.

More than one-third of newly formed *Ds39* elements (17 of 49) have filler DNA between the deletion endpoints (Figure 5). The presence at the deletion junctions of filler DNAs from nearby sequences suggests that the filler insertions are templated. They

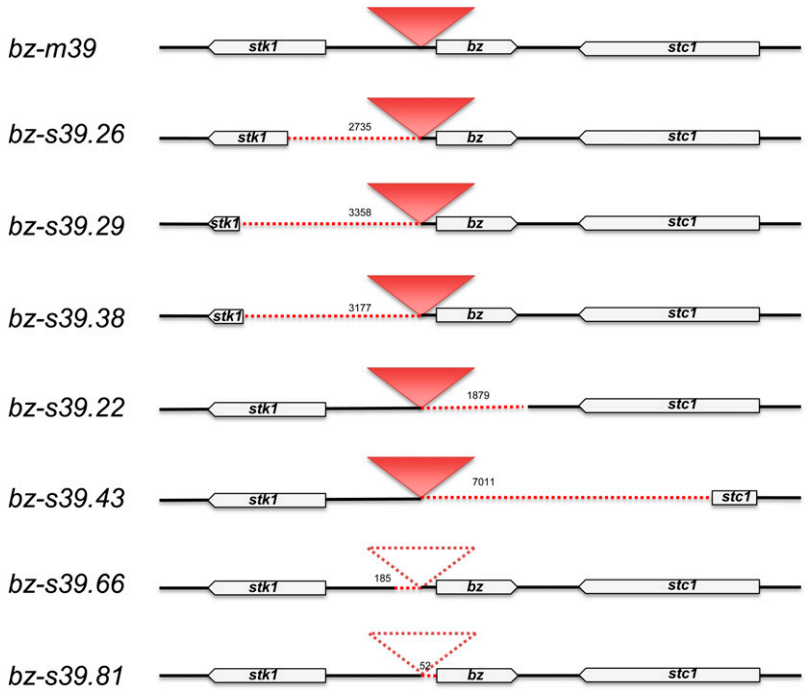

Figure 8. Structure of Adjacent Deletions.

Pentagons represent genic sequences, the solid triangle represents *Ac*, dotted lines represent gene sequence deletions, and the dotted triangle represents an excised *Ac*. The size of each deletion in bp is shown above the line. Adjacent deletions can occur at either end of *Ac* and may be accompanied by excision of *Ac*.
[See online article for color version of this figure.]

likely arise from misannealing to the sister chromatid during repair DNA synthesis. Multiple cycles of strand invasion occur during repair of the DSB: a short repair synthesis tract dissociates from its template, probes for its complementary sequences, and reinvades a template for strand extension when a complementary sequence is not found (McVey et al., 2004). When nascent DNA misanneals at a microhomology site, DNA synthesis would slow down, promoting the activity of alternative end joining DNA ligase I (Liang et al., 2008; Huefner et al., 2011), which ligates the two partially synthesized ends. In *Drosophila*, θ DNA polymerase has been speculated to create microhomologies that can be used during the annealing stage of the end joining when suitable microhomologies are not present (Chan et al., 2010). The above model for the formation of deletions and filler DNA is similar to one proposed by Yan et al. (1999) for the formation of new *Ds* elements. In that model, slip-mispairing during repair DNA synthesis between two short direct repeats would result in the deletion of one repeat and the sequence between the two repeats, yielding a new *Ds* element. A second slip-mispairing would explain the appearance of filler DNA (Yan et al., 1999), and sequential slips would explain filler DNA originating from multiple locations (Conrad et al., 2007).

A synthesis-dependent strand-annealing pathway was originally proposed to explain the formation of internal deletion derivatives of *P* after excision (Nassif et al., 1994) and the retention of a single LTR from a *copia* retrotransposon inserted between the two ends of a *P* element (Kurkulos et al., 1994). This mechanism has also been proposed to explain the formation of internal deletions of the *Mutator* transposon in maize (Lisch et al., 1995; Hsia and Schnable, 1996). However, the original synthesis-dependent strand-annealing model does not readily explain the frequent occurrence of filler DNA at the *Ds* and *fAc* deletion junctions reported here.

Terminal deletions of *Ac* or *fAc* elements are the second most abundant class of bz-s derivatives. Nine such alleles were recovered in our study, accounting for 15% of *Ac* mutations. The three instances of *fAc* elements reported in the literature retained the terminal 1.5- to 2.5-kb 3′ portion of *Ac* (Ralston et al., 1989; Zhang and Peterson, 1999; Conrad et al., 2007). Six of the nine *fAc*s recovered in this experiment also retained the 3′ end, but three retained the 5′ end instead, indicating that either end of *Ac* can be terminally deleted, although the 5′ end seems to be deleted more frequently. Four alleles have short host sequence duplications of 4 to 62 bp, whereas two others have larger adjacent deletions of either side. Both types can be explained by the model presented in Figure 9B. We propose that a *fAc* arises from an attempted, but failed, transposition to the *Ac* element on the sister chromatid, followed by microhomology-mediated repair synthesis of the DSB at the intended target site. There is no *Ac* template on the sister chromatid; therefore, repair of the DSB may begin with one end invading the sister chromatid at a site of microhomology near the *Ac* excision site, followed by DNA synthesis and eventual return to the original chromatid. This would give rise to a fractured or terminally deleted *Ac* and either

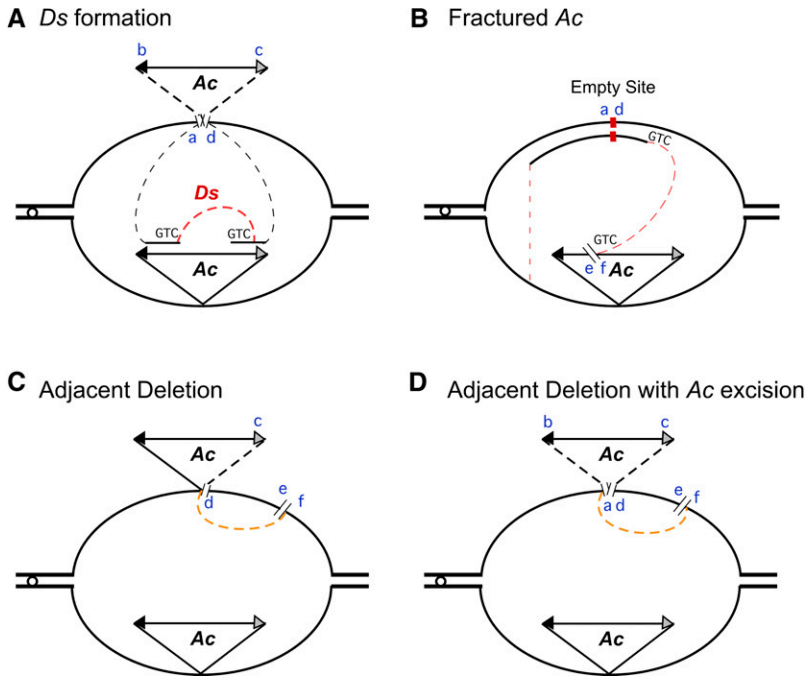

Figure 9. Models for the Origin of the Various *Ac* Mutations.

The diagrams illustrate DNA replication bubbles during chromosome replication and the aberrant repair of *Ac*-induced DSBs that leads to the formation of *Ac* mutations. The TE 5′ ends are represented as solid arrowheads, and the 3′ ends are represented as hatched ones. In each transposition reaction, the *Ac* transposase makes three cuts, one at each TE end to be mobilized and one at the receptor site, and generates six cut ends (a to f), as follows: a, host DNA adjacent to TE 5′ end; b, TE 5′ end; c, TE 3′ end; d, host DNA adjacent to TE 3′ end; e and f, host target site. The GTC trinucleotide sequences represent sites of microhomology in **(A)** and **(B)**. Red dotted lines represent synthesis-dependent MMEJ–mediated (**[A]** and **[B]**) mutational events, and orange dotted lines represent NHEJ–mediated (**[C]** and **[D]**) mutational events. The dotted lines in the *Ac* triangle (**[A]** and **[D]**) indicate discontinuity between *Ac* and the host chromosome.
(A) DSB repair of the *Ac* excision site is initiated with strand invasion of the sister chromatid by the a and d cut ends to begin copying *Ac*. MMEJ between the two GTC repeats leads to the formation of an internally deleted *Ds* element.
(B) In an aborted *Ac* transposition to the *Ac* element in the sister chromatid, the f end of the receptor site cut invades the sister chromatid at a site of microhomology (GTC) near the NHEJ-repaired a to d excision site. DNA repair synthesis and eventual return to the original chromatid result in the formation of a fractured *Ac* and a duplication of *Ac*-adjacent DNA.
(C) An aberrant transposition resulting from noncleavage or rejoining of the a to b site leads to the formation of a typical c to f transposition junction, but loss of the fragment between *Ac* and the e to f receptor site.
(D) An aberrant ligation of the host a and f cut ends at the excision and receptor sites, respectively, leads to loss of *Ac* and the fragment between *Ac* and the receptor site.

a duplication or deletion of adjacent DNA, depending on the location of the microhomology relative to the empty site. If the proposed transposition to the *Ac* element in the sister chromatid had resolved normally, a double *Ac* element would have resulted. Alleles carrying double *Ac* elements, such as *o2-m55* (Michel et al., 1994), produce mutable phenotypes, so a similar derivative of *bz-m39* would not have been selected in our experiment.

Of the few stable bz derivatives without rearrangements of transposon sequences, the most numerous are *Ac*-adjacent deletions. Transposon-adjacent deletions are common in bacteria and were first described for IS1 by Reif and Saedler (1975). Seven such alleles were recovered in our study, accounting for less than 10% of the bz-s mutations. Five of them retained *Ac* at the original location. They most likely arose from an incomplete *Ac* transposition of only one end of the transposon to a nearby site that results in the loss of sequences between that site and the original insertion site (Figure 9C). As in *bz-s:2114*(*Ac*) (Dooner et al., 1988), *Ac* is not flanked by an 8-bp TSD in any of these five *bz-s* alleles. Peculiarly, although adjacent inversions occur as frequently as adjacent deletions in bacteria, none were recovered in this study. Two alleles have adjacent deletions accompanied by an *Ac* excision. Such deletions constitute the most common type of excision product of the *P* element in *Drosophila* (Engels, 1989). They likely arose from an aborted transposition event to a nearby site followed by NHEJ (Figure 9D). The transposase cleaves at the original insertion site and the potential reinsertion site; however, the transposon fails to reinsert, and ligation of the two cut sites via NHEJ leads to loss of the sequences between them.

Identification of Additional Requirements for *Ac* Transposition

The analysis of loss-of-function derivatives from *bz-m39*(*Ac*) has uncovered previously unknown *trans* and *cis* requirements for *Ac* transposition. In derivative *bz-m39.55*, *Ac* has suffered a tiny

3-bp deletion that removes a Ser at position 305 and renders the transposase almost inactive, indicating that Ser-305 is important for activity. This residue is well conserved among *hAT* transposases of the *Ac*/*Tam3* clade (Robertson, 2002) and is found in some nonplant transposases, such as the human *Tramp* and the fungal *restless* clade (see Supplemental Figures 3A and 3B and Supplemental Data Set 1 online). The 4562-bp element in *bz-m39.55* transposes very rarely by itself, but normally in the presence of *Ac*, so only its *trans* function has been affected by the deletion.

In derivative *bz-s39.24*, *Ac* has undergone a 7-bp deletion of nucleotides 22 to 28 (AAAATCC) in the 5′ subterminal region that prevents it from transposing. It can still encode a functional transposase, behaving as an *Ac-im* (Conrad and Brutnell, 2005). The 11-bp TIR and multiple copies of the transposase binding A/TCGG subterminal repeat were known to be essential for excision (Kunze and Starlinger, 1989; Becker and Kunze, 1997; Kunze and Weil, 2002), but the deleted sequence is not a part of either. Thus, the analysis of the nontransposing element in *bz-s39.24* identifies a new *cis* requirement for *Ac* transposition, which could be either the deleted sequence itself or simply a change in the spacing between the TIR and the subterminal repeats where the transposase binds.

METHODS

Genetic Stocks

All the stocks used in this study shared the common genetic background of the inbred W22. The *bronze* alleles and the aleurone phenotypes of the various stocks are described below.

bz-m39(*Ac*) (heavy purple spots on a bronze background): a mutable allele harboring an *Ac* element in the 5′ UTR of the *Bz-McC* allele, at a position 39 to 32 bp upstream of the start codon. The 8-bp span refers to the location of the *bz* TSD on either side of *Ac*. The simple transposon excisions from this site restore gene function. This allele was recovered from a reinsertion of *Ac2094* into the *bz* locus in the same experiment described by Yan et al. (1999) for the isolation of *bz-m41* and *bz-m43*.

Bz-McC (purple): the normal progenitor allele of the *bz-m39*(*Ac*) and *bz-m2*(*Ac*) mutations.

bz-m2(*Ac*) (purple spots on a bronze background): an allele that arose from the insertion of the 4.6-kb *Ac* element at position 755 to 762 in the second exon of *Bz-McC* (McClintock, 1955; Ralston et al., 1988). Most transposon excisions from this site fail to restore gene function (Dooner and Belachew, 1989).

bz-m2(*D1*) (bronze in the absence of *Ac*, spotted in its presence): the first derivative from *bz-m2*(*Ac*), harboring a 3.3-kb internally deleted *Ds* element at the same position as *Ac* in *bz-m2*(*Ac*) (McClintock, 1962; Dooner et al., 1986).

sh-bz-X2 (shrunken, bronze): an x-ray–induced deletion of a large chromosomal fragment that includes *sh*, *bz*, and other loci between *sh* and *bz*, such as *stc1* (Mottinger, 1973; Fu et al., 2001).

wx-m7(*Ac*) (waxy endosperm with sectors of nonwaxy revertant tissue): an unstable *wx* allele described by McClintock (1964). It arose by insertion of the 4.6-kb *Ac* element in the 5′ UTR of the *Wx* gene (Müller-Neumann et al., 1984; Klösgen et al., 1986).

Selection and Analysis of Bz′ and bz-s Derivatives

Bz′′ and bz-s derivatives were isolated from testcrosses of *Sh bz-m39*(*Ac*) *wx/sh-bz-X2 wx* heterozygotes to *sh-bz-X2 wx*. In these crosses, the two parental kernel classes are plump, spotted and shrunken, bronze. *sh* and *bz* cannot recombine in the hemizygous deletion parent; therefore, exceptional plump, purple (Bz′) kernels represent *Bz′* derivatives from *bz-m39*(*Ac*), and plump, stable bronze (bz-s) kernels represent bz-s derivatives. *bz-m39*(*Ac*) as female parent produces very heavily spotted kernels, making it hard to differentiate purple from spotted kernels. Therefore, the whole population was planted, and those seedlings with solid purple coleoptiles were selected as *Bz′* derivatives. *bz-s* derivatives were first screened by three diagnostic PCR reactions (as described in Results) to identify different types of deletion mutations and were then crossed to *wx-m7*(*Ac*) to determine the mobility of the element. A selected group was crossed to *bz-m2*(*D1*) to score for *Ac* activity (see Results).

DNA Extraction, Blotting, and Hybridization

Leaf DNA for DNA gel blot hybridization was isolated by a urea extraction procedure (Greene et al., 1994). A modified cetyltrimethylammonium bromide extraction method (Huang and Dooner, 2008) was used for the large number of DNA preparations required for PCR and sequencing analysis. Restriction digested DNA (10 μg) was resolved on 0.8% agarose gels and transferred to Hybond XL nylon membranes (Amersham Biosciences). ^{32}P-labeled probes were generated with Ready-To-Go DNA labeling beads (Amersham Biosciences). The 740-bp *Ac* probe was amplified from a genomic clone using primers in exon 2 (CACACTGG-CCAAAGGTTATCACA) and exon 3 (TCATTGCAACGGCCATTCTCCTAA) of the *Ac* transposase gene.

PCR, Inverse PCR, and Sequencing

PCR was performed according to the protocol of QiaTaq (Qiagen). Long-strand DNA fragment amplification was performed according to the protocol of Roche Expand Long Range (Hoffmann-La Roche). PCR products were cloned into pGEM-T Easy Vector (Promega) and transformed into XL-Blue competent cells. Plasmids were purified with a Qiagen Spin Miniprep Kit. DNA sequencing of plasmids or PCR products was performed in an ABI 3730 sequencer (Perkin-Elmer) following the manufacturer's instructions. Primers used in this work are shown in Supplemental Table 1 online.

Phylogenetic Analysis

The *Ac* sequence was queried against the GenBank nr protein databases, excluding searches from *Zea*. Sample hits from different species were chosen for further analysis. Some *hAT* transposons of the more distant groups (Robertson, 2002; Xu and Dooner, 2005) were also incorporated. To reduce the redundancy within the data, sequences with a high degree of similarity to another sequence from the same species were eliminated so that only one of them was included in the comparison. The full-length amino acid sequences were aligned by Clustal Omega (http://www.clustal.org/omega/). A phylogenetic tree was constructed using neighbor joining in MEGA version 5.05 (http://www.megasoftware.net/), with 1000 bootstrap replicates and the pairwise-deletion option for handling gaps.

Accession Numbers

Sequence data from this article can be found in the GenBank/EMBL databases under the following accession numbers: *Ac* sequence (GenBank X05425), McC *bz* haplotype contig (GenBank AF391808), *bz-m39* (*Ac*) and its *bz* derivatives (GenBank JX910919 to JX910943).

Supplemental Data

The following materials are available in the online version of this article.

Supplemental Figure 1. Excision Footprints among Bz′ Revertants Recovered from Female and Male Gametes.

Supplemental Figure 2. *bz-m39.31* Phenotype.

Supplemental Figure 3. Sequence Conservation among *hAT* Transposases.

Supplemental Figure 4. Methylation of Inactive *Ac* in *bz-c39.27*.

Supplemental Table 1. Primers Used in This Work.

Supplemental Data Set 1. Text File of Alignment Corresponding to Phylogenetic Tree in Supplemental Figure 3 Online.

ACKNOWLEDGMENTS

We thank Yubin Li and Qinghua Wang for comments on the article and Yubin Li for part of Figure 1. This research was supported by a Charles and Johanna Busch Predoctoral Fellowship and a Busch-Waksman Postdoctoral Fellowship to J.T.H. and by National Science Foundation grant DBI-0929350 to H.K.D.

AUTHOR CONTRIBUTIONS

J.T.H. and H.K.D. designed the work, performed the research, analyzed the data, and wrote the article.

Received August 20, 2012; revised September 21, 2012; accepted October 9, 2012; published October 30, 2012.

REFERENCES

Becker, H.A., and Kunze, R. (1997). Maize *Activator* transposase has a bipartite DNA binding domain that recognizes subterminal sequences and the terminal inverted repeats. Mol. Gen. Genet. **254:** 219–230.

Brutnell, T.P., and Dellaporta, S.L. (1994). Somatic inactivation and reactivation of Ac associated with changes in cytosine methylation and transposase expression. Genetics **138:** 213–225.

Chan, S.H., Yu, A.M., and McVey, M. (2010). Dual roles for DNA polymerase theta in alternative end-joining repair of double-strand breaks in *Drosophila*. PLoS Genet. **6:** e1001005.

Chomet, P.S., Wessler, S., and Dellaporta, S.L. (1987). Inactivation of the maize transposable element *Activator* (*Ac*) is associated with its DNA modification. EMBO J. **6:** 295–302.

Conrad, L.J., Bai, L., Ahern, K., Dusinberre, K., Kane, D.P., and Brutnell, T.P. (2007). State II *dissociation* element formation following *activator* excision in maize. Genetics **177:** 737–747.

Conrad, L.J., and Brutnell, T.P. (2005). Ac-immobilized, a stable source of Activator transposase that mediates sporophytic and gametophytic excision of Dissociation elements in maize. Genetics **171:** 1999–2012.

Coupland, G., Baker, B., Schell, J., and Starlinger, P. (1988). Characterization of the maize transposable element *Ac* by internal deletions. EMBO J. **7:** 3653–3659.

Coupland, G., Plum, C., Chatterjee, S., Post, A., and Starlinger, P. (1989). Sequences near the termini are required for transposition of the maize transposon *Ac* in transgenic tobacco plants. Proc. Natl. Acad. Sci. USA **86:** 9385–9388.

Cowperthwaite, M., Park, W., Xu, Z., Yan, X., Maurais, S.C., and Dooner, H.K. (2002). Use of the transposon *Ac* as a gene-searching engine in the maize genome. Plant Cell **14:** 713–726.

Dooner, H.K., and Belachew, A. (1989). Transposition pattern of the maize element *Ac* from the *bz-m2*(*Ac*) allele. Genetics **122:** 447–457.

Dooner, H.K., English, J., and Ralston, E.J. (1988). The frequency of transposition of the maize element Activator is not affected by an adjacent deletion. Mol. Gen. Genet. **211:** 485–491.

Dooner, H.K., English, J., Ralston, E., and Weck, E. (1986). A single genetic unit specifies two transposition functions in the maize element *activator*. Science **234:** 210–211.

Dooner, H.K., and Weil, C.F. (2013). Transposons and gene creation. In Plant Transposons and Genome Dynamics in Evolution, N.V. Fedoroff, ed (Hoboken, NJ: John Wiley & Sons), in press.

Engels, W.R. (1989). P elements in *Drosophila melanogaster*. In Mobile DNA, D. Berg and M. Howe, eds (Washington, D.C.: American Society for Microbiology Press), pp. 437–484.

Fedoroff, N.V., Furtek, D.B., and Nelson, O.E. Jr. (1984). Cloning of the *bronze* locus in maize by a simple and generalizable procedure using the transposable controlling element *Activator* (*Ac*). Proc. Natl. Acad. Sci. USA **81:** 3825–3829.

Fu, H., Park, W., Yan, X., Zheng, Z., Shen, B., and Dooner, H.K. (2001). The highly recombinogenic *bz* locus lies in an unusually gene-rich region of the maize genome. Proc. Natl. Acad. Sci. USA **98:** 8903–8908.

Greene, B., Walko, R., and Hake, S. (1994). Mutator insertions in an intron of the maize *knotted1* gene result in dominant suppressible mutations. Genetics **138:** 1275–1285.

Hehl, R., and Baker, B. (1989). Induced transposition of *Ds* by a stable *Ac* in crosses of transgenic tobacco plants. Mol. Gen. Genet. **217:** 53–59.

Hsia, A.P., and Schnable, P.S. (1996). DNA sequence analyses support the role of interrupted gap repair in the origin of internal deletions of the maize transposon, MuDR. Genetics **142:** 603–618.

Huang, J.T., and Dooner, H.K. (2008). Macrotransposition and other complex chromosomal restructuring in maize by closely linked transposons in direct orientation. Plant Cell **20:** 2019–2032.

Huefner, N.D., Mizuno, Y., Weil, C.F., Korf, I., and Britt, A.B. (2011). Breadth by depth: Expanding our understanding of the repair of transposon-induced DNA double strand breaks via deep-sequencing. DNA Repair (Amst.) **10:** 1023–1033.

Klösgen, R.B., Gierl, A., Schwarz-Sommer, S., and Saedler, H. (1986). Molecular analysis of the *waxy* locus of *Zea mays*. Mol. Gen. Genet. **203:** 237–244.

Kunze, R., and Starlinger, P. (1989). The putative transposase of transposable element *Ac* from *Zea mays* L. interacts with subterminal sequences of *Ac*. EMBO J. **8:** 3177–3185.

Kunze, R., and Weil, C.F. (2002). The *hAT* and CACTA superfamilies of plant transposons. In Mobile DNA II, N.L. Craig, R. Craigie, M. Gellert, and A.M. Lambowitz, eds (Washington, D.C.: American Society for Microbiology Press), pp. 565–610.

Kurkulos, M., Weinberg, J.M., Roy, D., and Mount, S.M. (1994). P element-mediated in vivo deletion analysis of white-apricot: Deletions between direct repeats are strongly favored. Genetics **136:** 1001–1011.

Liang, L., Deng, L., Nguyen, S.C., Zhao, X., Maulion, C.D., Shao, C., and Tischfield, J.A. (2008). Human DNA ligases I and III, but not ligase IV, are required for microhomology-mediated end joining of DNA double-strand breaks. Nucleic Acids Res. **36:** 3297–3310.

Lisch, D., Chomet, P., and Freeling, M. (1995). Genetic characterization of the *Mutator* system in maize: Behavior and regulation of *Mu* transposons in a minimal line. Genetics **139:** 1777–1796.

McClintock, B. (1949). Mutable loci in maize. Carnegie Inst. Wash. Yrbk. **48:** 142–154.

McClintock, B. (1955). Controlled mutation in maize. Carnegie Inst. Wash. Yrbk. **54:** 245–255.

McClintock, B. (1956). Mutation in maize. Carnegie Inst. Wash. Yrbk. **55:** 323–332.

McClintock, B. (1962). Topographical relations between elements of control systems in maize. Carnegie Inst. Wash. Yrbk. **61:** 448–461.

McClintock, B. (1963). Further studies of gene-control systems in maize. Carnegie Inst. Wash. Yrbk. **62:** 486–493.

McClintock, B. (1964). Aspects of gene regulation in maize. Carnegie Inst. Wash. Yrbk. **63:** 592–602.

McVey, M., Adams, M., Staeva-Vieira, E., and Sekelsky, J.J. (2004). Evidence for multiple cycles of strand invasion during repair of double-strand gaps in *Drosophila*. Genetics **167:** 699–705.

Michel, D., Salamini, F., Motto, M., and Döring, H.-P. (1994). An unstable allele at the maize *Opaque2* locus is caused by the insertion of a double *Ac* element. Mol. Gen. Genet. **243:** 334–342.

Mottinger, J.P. (1973). Unstable mutants of *bronze* induced by premeiotic X-ray treatment in maize. Theor. Appl. Genet. **43:** 190–195.

Müller-Neumann, M., Yoder, J.I., and Starlinger, P. (1984). The DNA sequence of the transposable element *Ac* of *Zea mays* L. Mol. Gen. Genet. **198:** 19–24.

Nassif, N., Penney, J., Pal, S., Engels, W.R., and Gloor, G.B. (1994). Efficient copying of nonhomologous sequences from ectopic sites via P-element-induced gap repair. Mol. Cell. Biol. **14:** 1613–1625.

Pohlman, R.F., Fedoroff, N.V., and Messing, J. (1984). The nucleotide sequence of the maize controlling element *Activator*. Cell **37:** 635–643.

Ralston, E.J., English, J., and Dooner, H.K. (1989). Chromosome-breaking structure in maize involving a fractured *Ac* element. Proc. Natl. Acad. Sci. USA **86:** 9451–9455.

Ralston, E.J., English, J.J., and Dooner, H.K. (1988). Sequence of three *bronze* alleles of maize and correlation with the genetic fine structure. Genetics **119:** 185–197.

Reif, H.J., and Saedler, H. (1975). IS1 is involved in deletion formation in the gal region of *E. coli* K12. Mol. Gen. Genet. **137:** 17–28.

Robertson, H.M. (2002). Evolution of DNA transposons in eukaryotes. In Mobile DNA II, N.L. Craig, R. Craigie, M. Gellert, and A.M. Lambowitz, eds (Washington, D.C.: American Society for Microbiology Press), pp. 1093–1110.

Roth, D.B., Chang, X.B., and Wilson, J.H. (1989). Comparison of filler DNA at immune, nonimmune, and oncogenic rearrangements suggests multiple mechanisms of formation. Mol. Cell. Biol. **9:** 3049–3057.

Roth, D.B., and Wilson, J.H. (1985). Relative rates of homologous and nonhomologous recombination in transfected DNA. Proc. Natl. Acad. Sci. USA **82:** 3355–3359.

Rubin, E., and Levy, A.A. (1997). Abortive gap repair: Underlying mechanism for *Ds* element formation. Mol. Cell. Biol. **17:** 6294–6302.

Sainsard-Chanet, A., and Begel, O. (1990). Insertion of an LrDNA gene fragment and of filler DNA at a mitochondrial exon-intron junction in *Podospora*. Nucleic Acids Res. **18:** 779–783.

Schwartz, D., and Dennis, E. (1986). Transposase activity of the *Ac* controlling element in maize is regulated by its degree of methylation. Mol. Gen. Genet. **205:** 476–482.

Scott, L., LaFoe, D., and Weil, C.F. (1996). Adjacent sequences influence DNA repair accompanying transposon excision in maize. Genetics **142:** 237–246.

Wessler, S., Tarpley, A., Purugganan, M., Spell, M., and Okagaki, R. (1990). Filler DNA is associated with spontaneous deletions in maize. Proc. Natl. Acad. Sci. USA **87:** 8731–8735.

Xiao, Y.L., and Peterson, T. (2002). Ac transposition is impaired by a small terminal deletion. Mol. Genet. Genomics **266:** 720–731.

Xu, Z., and Dooner, H.K. (2005). *Mx-rMx*, a family of interacting transposons in the growing *hAT* superfamily of maize. Plant Cell **17:** 375–388.

Yan, X., Martínez-Férez, I.M., Kavchok, S., and Dooner, H.K. (1999). Origination of *Ds* elements from *Ac* elements in maize: Evidence for rare repair synthesis at the site of *Ac* excision. Genetics **152:** 1733–1740.

Yu, A.M., and McVey, M. (2010). Synthesis-dependent microhomology-mediated end joining accounts for multiple types of repair junctions. Nucleic Acids Res. **38:** 5706–5717.

Zhang, J., and Peterson, T. (1999). Genome rearrangements by nonlinear transposons in maize. Genetics **153:** 1403–1410.

Zhang, J., and Peterson, T. (2004). Transposition of reversed Ac element ends generates chromosome rearrangements in maize. Genetics **167:** 1929–1937.